Mon. Not. R. Astron. Soc. **364,** 649–653 (2005) doi:10.1111/j.1365-2966.2005.09587.x

The effect of condensates on the characterization of transiting planet atmospheres with transmission spectroscopy

Jonathan J. Fortney★

Space Science and Astrobiology Division, NASA Ames Research Center, MS 245-3, Moffett Field, CA 94035, USA

Accepted 2005 September 3. Received 2005 August 16; in original form 2005 June 10

ABSTRACT

Through a simple physical argument we show that the slant optical depth through the atmosphere of a 'hot Jupiter' planet is ∼35–90 times greater than the normal optical depth. This not unexpected result has direct consequences for the method of transmission spectroscopy for characterizing the atmospheres of transiting giant planets. The atmospheres of these planets likely contain minor condensates and hazes, which at normal viewing geometry have negligible optical depth, but at slant viewing geometry have appreciable optical depth that can obscure absorption features of gaseous atmospheric species. We identify several possible condensates. We predict that this is a general masking mechanism for all planets, not just for HD 209458b, and will lead to weaker than expected or undetected absorption features. Constraints on an atmosphere from transmission spectroscopy are not the same as constraints on an atmosphere at normal viewing geometry.

Key words: radiative transfer – planetary systems.

1 INTRODUCTION

To date, eight extrasolar giant planets (EGPs) are known to transit their parent stars in tight, several day orbits. Characterizing the atmospheres of two of these planets (HD 209458b and TrES-1) has been a major goal for many astronomers in the past few years. Not long after the discovery of the transits of planet HD 209458b (Charbonneau et al. 2000; Henry et al. 2000), a number of studies appeared in the literature on radiative transfer aspects of 'Pegasi planet' (or 'hot Jupiter') transits, namely, how stellar light passing through a planet's atmosphere can be absorbed at wavelengths where opacity is high. This would lead a distant observer who obtained a spectrum of the star during a transit of the planet to see the planet's atmospheric absorption spectrum superimposed on the star's spectrum. The physics behind this process was laid out theoretically and modelled by Seager & Sasselov (2000), Brown (2001) and Hubbard et al. (2001). The consensus of these three studies was that for HD 209458b, for a clear, cloudless atmosphere, the transit depth (0.016 in relative flux) could itself vary by up to a few per cent due to absorption by gaseous sodium, potassium, water and carbon monoxide.

Shortly thereafter Charbonneau et al. (2002) used the Space Telescope Imaging Spectrograph (STIS) instrument aboard *Hubble Space Telescope* (*HST*) to observe the predicted sodium absorption doublet at 589 nm. However, the magnitude of this absorption was 2–3 times weaker than had been predicted by theoretical models that assumed a clear and cloudless atmosphere. A number of possible reasons for this discrepancy were put forth in Charbonneau et al. (2002), including a global underabundance of sodium, ionization of sodium by stellar flux, sodium being tied up in condensates or molecules (see also Atreya et al. 2003) or high clouds obscuring the absorption of sodium (see also Seager & Sasselov 2000). In addition, Barman et al. (2002) found that neutral atomic sodium may be out of local thermodynamic equilibrium, leading to a deficit of sodium atoms able to absorb at 589 nm, relative to local thermodynamic equilibrium (LTE) calculations. Fortney et al. (2003) derived a self-consistent pressure–temperature (*P–T*) profile for HD 209458b, and found that silicate and iron clouds reside high in the planet's atmosphere, at the several millibar level, and that these opaque clouds mask the absorption of sodium enough to match the Charbonneau et al. (2002) observations. However, as noted by the authors at the time, this conclusion is extremely sensitive to the *P–T* profile calculated for the atmosphere. Recently, Iro, Bezard & Guillot (2005) have shown that a substantial day–night temperature contrast in the planet's atmosphere could lead to a sink of atomic sodium, as the atom could be tied up into the condensate Na_2S on the planet's night side.

In addition to the sodium observation, Deming et al. (2005) have recently attempted to observe absorption due to first overtone bands of CO at ∼2.3 μm, using Near-Infrared Spectrograph (NIRSPEC) on the Keck Telescope. Their sensitively was high enough such that if CO was present in the abundances predicted for a clear and cloud-free atmosphere, the CO should have been detected. However, it was not, and the authors point to the masking effect of high clouds as the likely culprit. Currently, other searches are underway to detect the absorption of H_2O (Harrington et al. 2002) and H_3^+ (Haywood et al. 2004) in the atmosphere of HD 209458b. Narita et al. (2005)

★E-mail: jfortney@arc.nasa.gov

have also reported upper limits due to absorption by Li, H, Fe and Ca. These studies are in addition to the exosphere absorption studies such as Vidal-Madjar et al. (2003, 2004), which have yielded important results, but are not the subject of our study here.

To date, there has been no discussion in the extrasolar planets literature regarding how condensates less abundant than the 'standard' brown dwarf condensates (such as silicates and iron) may effect transmission spectroscopy. In the following sections, we show that condensates that may have insignificant optical depth when viewed at normal geometry can have appreciable optical depths for the *slant* viewing geometry relevant for transits. Searches for transmission absorption features in the atmosphere of HD 209458b, or any other similar searches for absorption during transits of other planets in the future, will very likely find weak or non-existent absorption features. Constraints on atmospheric abundances derived from transmission spectroscopy will not map directly as constraints on abundances under normal viewing geometry.

2 GEOMETRY OF THE PROBLEM

The studies of Hubbard et al. (2001) and Fortney et al. (2003) showed that the pressures probed by transit observations are a sensitive function of wavelength. Specifically for HD 209458b, Fortney et al. (2003) showed that in the spectral region from 580 to 640 nm, which spanned the Charbonneau et al. (2002) observations, the pressure where the slant optical depth reached 1 varied from a few microbars near the sodium line cores to potentially 50 mbar at 640 nm, if the atmosphere was clear. This pressure could reach nearly a few hundred millibars at wavelengths of relatively low opacity.

At these low pressures it is reasonable, to the first order, to approximate the atmosphere as having a constant temperature with height. If a planet's atmosphere is in hydrostatic equilibrium, with a constant temperature and mean molecular weight, then the barotropic law holds, which states (Chamberlain & Hunten 1987)

$$p(r) = p(r_0)\exp\left[-\frac{GMm}{kTrr_0}(r - r_0)\right], \tag{1}$$

where p is the pressure, r is the radius of interest, r_0 is the reference radius, G is the gravitational constant, M is the mass of the planet, m is the mean mass of a molecule in the atmosphere, k is Boltzmann's constant and T is the temperature. The vertical integrated column density of the atmosphere $N_{\rm V}(r_0)$, above a given local density $n(r_0)$, is given by

$$N_{\rm V}(r_0) \equiv \int_{r_0}^{\infty} n(r)\mathrm{d}r = \int_0^{p(r_0)} \frac{r^2}{GMm}\mathrm{d}p \approx \frac{p(r_0)}{g(r_0)m} = n(r_0)H, \tag{2}$$

where H is the scaleheight ($H = kT/mg$) and g is the planet's gravitational acceleration. Clearly, if our reference density is n_0, our column density is then n_0H. With the assumption that g is constant in the atmosphere, equation (1) can be simplified to

$$p(z) \approx p(z_0)\exp\left(-\frac{z - z_0}{H}\right), \tag{3}$$

where we have replaced the two radii, r and r_0 with heights from a given level, z and z_0, respectively.

We now turn to Fig. 1. Here a is a given radius of the planet, say where the normal optical depth is unity. The thickness of our atmosphere is z and x is a line tangential to our optical depth unity 'surface', horizontal to the horizon. Using the Pythagorean theorem and $2az \gg z^2$, then $z \approx x^2/2a$. Therefore, equation (3), when written in terms of density, rather that pressure, becomes

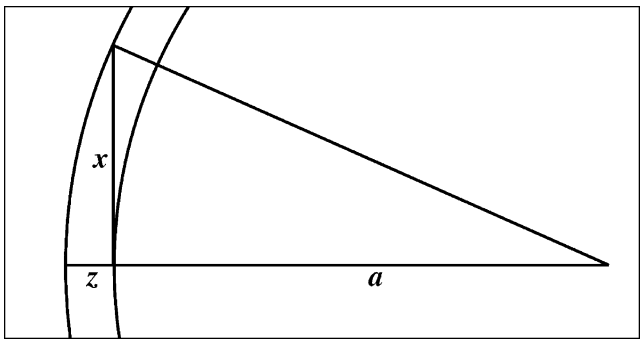

Figure 1. Diagram of slant versus normal geometry. a is the planet's radius out to a standard level, say the radius at normal optical depth unity. z is the thickness of the atmosphere above this level, out to some very low pressure. x is the distance to this same low pressure, towards the horizon.

$$n(x) = n_0\exp\left(\frac{-x^2}{2aH}\right) \tag{4}$$

and the horizontal integrated density $N_{\rm H}$, from horizon to horizon, is

$$N_{\rm H} = \int_{-\infty}^{\infty} n(x)\mathrm{d}x = n_0\sqrt{2\pi aH}. \tag{5}$$

The ratio of the horizontal integrated density to the vertical integrated density is the quantity of interest here. This quantity, which we will label η, simplifies to

$$\eta = \frac{N_{\rm H}}{N_{\rm V}} = \frac{\tau_{\rm H}}{\tau_{\rm V}} = \sqrt{\frac{2\pi a}{H}}. \tag{6}$$

This shows that the horizontal integrated density is significantly larger that the vertical integrated density. This ratio is ∼75 for Earth (and ∼128 for Jupiter), and leads to an atmosphere that has significantly different absorption and scattering properties at a *slant* geometry than for *normal* geometry, which one can easily observe at sunset. Since the optical depth is directly proportional to the column density, η is also the ratio of the slant optical depth to the normal optical depth.

3 APPLICATION TO EGPS

3.1 Atmospheric properties

For HD 209458b, assuming $T = 1200$ K, $a = 10^5$ km, and mean molecular weight $\mu = 2.3$, we find $\eta = 38$. For TrES-1, which although similar in mass has a 30 per cent smaller radius and is ∼300 K colder in effective temperature (Fortney et al. 2005); we find $\eta = 50$. A minor condensate, having a normal optical depth of 0.02, which would be easily ignored when calculating a planet's emission or reflection spectrum, would have an optical depth of 1 in slant transmission through the planet's atmosphere.

In Fig. 2, we plot self-consistent *P–T* profiles for planets HD 209458b and TrES-1, as taken from Fortney et al. (2005). Also plotted are condensation curves for a variety of equilibrium condensates, spanning a large range in temperature. The condensation curves are taken from Lodders & Fegley (2005). We note that the *P–T* profile shown here for HD 209458b is cooler than that of Fortney et al. (2003) because here we assume the planet is able to reradiate absorbed stellar flux over the entire planet, whereas Fortney et al.

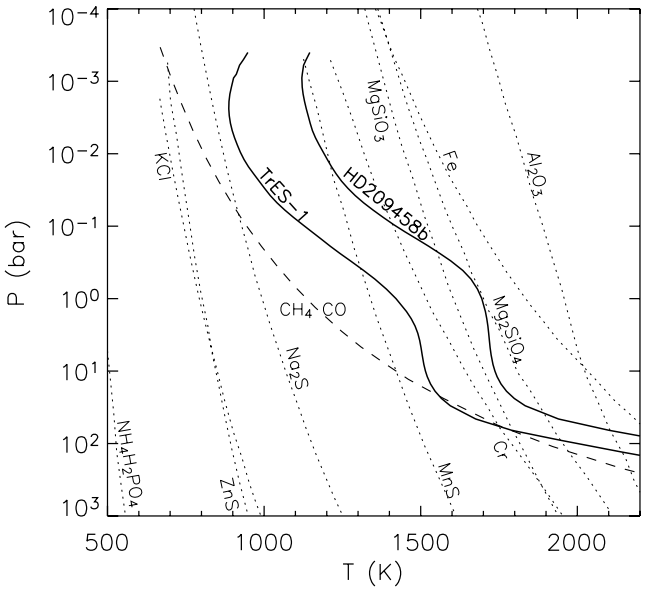

Figure 2. Pressure–temperature profiles for TrES-1 and HD 209458b. Condensation curves for various compounds, as taken from Lodders & Fegley (2005) are shown as dotted lines. The boundary where CH_4 and CO have the same abundance is shown as a dashed line.

(2003) assumed this reradiation could only occur on the planet's day side, leading to a warmer day side *P–T* profile. In addition, Fortney et al. (2003) utilized a different model atmosphere program (see Sudarsky, Burrows & Hubeny 2003).

We have used the transit radiative transfer program described in Hubbard et al. (2001) and Fortney et al. (2003) to compute both the normal optical depth and slant optical depth at various pressures in the atmosphere of both planets. This code takes a computed model atmosphere, for which T, P, ρ and extinction cross-sections are known as functions of altitude, under the assumption of hydrostatic equilibrium, and places the atmosphere on to an opaque disc of a given radius. Normal and slant optical depths are then computed numerically through the atmosphere. For isothermal atmospheres, we recover the same ratio η we calculated analytically, within less than ∼1 per cent. For the atmospheres we consider here, our pressure range of interest is the upper troposphere, and temperature decreases with altitude. Integrating upwards in altitude from a pressure of 1 bar, we calculate $\eta = 30$ for HD 209458b and 40 for TrES-1, in about 80 per cent of our simple analytic case. However, integrating from a lower pressure, say 10 mbar, may be more relevant, and from this pressure we calculate $\eta = 35.5$ for HD 209458b and 47 for TrES-1, which is ∼94 per cent of the value obtained from our simple analytical treatment. In summary, a more detailed analysis gives ratios of the slant optical depth to normal optical depth for these atmospheres that are consistent with our earlier simple analysis. These values are collected in Table 1.

3.2 Condensate scaleheight

The values for η calculated so far assume that the scaleheight for the condensate is the same as the scaleheight of the surrounding gas. However, there is strong evidence in the Jupiter's atmosphere that its visible ammonia cloud is more compact than the surrounding gas. Using *Voyager* infrared spectra Carlson, Lacis & Rossow (1994) derived a ratio of the scaleheight of condensate ($H_{\rm cond}$) to scaleheight of gas (H) of 0.35 ± 0.10 for equatorial zones and 0.40 ± 0.10 for northern tropical zones. Observations of the Jovian tropics with the *Infrared Space Observatory* by Brooke et al. (1998) indicate a scaleheight ratio of 0.3.

Table 1. Quantities of interest for various planets.

Planet	a (km)	H (km)	η	$H_{\rm cond}$ (km)	$\eta_{\rm cond}^{\star}$
Earth	6400	7	76	2.3	132
Jupiter	70 000	27	128	9	221
HD 209458b	100 000	440	38	747	66
TrES-1	75 000	185	50	62	87

*Value for $H_{\rm cond}$ and $\eta_{\rm cond}$ (condensate) are computed assuming $H_{\rm cond} = 1/3\ H$.

Further evidence for clouds of small vertical extent comes from observations of L-type stars and brown dwarfs, which have silicate and iron clouds in their visible atmospheres. The observed spectra of these objects have been accurately modelled by Marley et al. (2002) and Marley, Cushing & Saumon (2005) using the 1D cloud model of Ackerman & Marley (2001) with a sedimentation efficiency parameter, $f_{\rm sed} = 2$–3. This $f_{\rm sed}$ range gives silicate and iron clouds with $H_{\rm cond}/H = 0.25$–0.30 (Ackerman & Marley 2001). These observations and models indicate that equilibrium condensates, across a wide range of temperatures and chemical species, have scaleheights that are ∼1/3 of the local gas scaleheight. This leads to values of η that are ∼75 per cent larger than calculated earlier. Values of η would then increase to 66 for HD 209458b and 87 for TrES-1.

3.3 Minor condensates and hazes

For brown dwarf atmospheres, corundum (Al_2O_3), iron (Fe) and silicates ($MgSiO_3$ and/or Mg_2SiO_4) appear to be the only condensates that have appreciable optical depth, and therefore leave some imprint on the spectra of these objects (see, for instance, Ackerman & Marley 2001; Allard et al. 2001; Marley et al. 2002; Cooper et al. 2003; Lodders & Fegley 2005). However, at slant viewing geometry, one likely has to consider condensates that may be a factor of 100–1000 less abundant, compared to the silicates. From the work of (Fegley & Lodders 1994) on condensation in the deep atmospheres of Jupiter and Saturn and Lodders (2003) on the condensation temperatures of the elements, we can highlight condensates that fit into this abundance range. In order of decreasing condensation temperature, these are Cr, MnS, Na_2S, ZnS, KCl and $NH_4H_2PO_4$. These are the condensation curves plotted in Fig. 2.

To analyse the potential optical depths of these species, we will closely follow the analysis of Marley (2000), who derived an expression for the maximum optical depth of condensates in substellar atmospheres. We will use this equation to determine the relative optical depths of various species. This expression is

$$\tau_\lambda = 75\epsilon Q_\lambda(r_{\rm c})\varphi \left(\frac{P_{\rm c}}{1\ {\rm bar}}\right)\left(\frac{10^5\ {\rm cm\ s^{-2}}}{g}\right)\left(\frac{1\ \mu{\rm m}}{r_{\rm c}}\right)\left(\frac{1.0\ {\rm g\ cm^{-3}}}{\rho_{\rm c}}\right), \quad (7)$$

where ϵ is a factor $\leqslant 1$, which accounts for the finite amount of species left over after condensation, because of the vapour pressure above the condensate, Q_λ is the wavelength-dependent extinction efficiency from Mie theory, $r_{\rm c}$ is the radius of the condensate particles and $\varphi = f m_{\rm c}/\bar{m}$, where f is the mixing ratio of the species, $m_{\rm c}$ is the molecular weight of the condensed species and $\bar{m}$ is the mean molecular weight of the atmosphere. Additionally, $P_{\rm c}$ is the condensation pressure, g is gravitational acceleration in the

Table 2. Optical depths (at a wavelength of 1 μm) of lesser condensates in HD 209458b, for an atmosphere of solar composition.

Condensate	Molecular weight	Limiting species	f	Normal τ	Slant τ
$MgSiO_3$	100.4	Si/Mg	7×10^{-5}	0.5	33
Na_2S	78.1	Na	2×10^{-6}	0.011	0.73
$NH_4H_2PO_4$	113	P	5.8×10^{-7}	0.011	0.73
MnS	87	Mn	6.3×10^{-7}	0.0093	0.61
Cr	85	Cr	8.8×10^{-7}	0.0077	0.51
KCl	74.6	K	2.5×10^{-7}	0.0028	0.18
ZnS	97.5	Zn	8.5×10^{-8}	0.0014	0.09

atmosphere and ρ_c is the mass density of the condensate. Since at this point we are only interested in the *relative* optical depths of the various species at a given P_c, we will make several simplifications. Following Marley, we assume that ϵ, Q_λ, r_c and ρ_c are approximately equal for the condensate species, then the optical depth ratio for given condensates 1 and 2 reduces to

$$\frac{\tau_1}{\tau_2} = \frac{f_1 m_{c1}}{f_2 m_{c2}}. \quad (8)$$

For illustrative purposes, we used a *P–T* profile for HD 209458b that is slightly warmer than that shown in Fig. 2, along with the Ackerman & Marley (2001) cloud model with $f_{sed} = 2$, to compute the normal optical depth of a $MgSiO_3$ cloud with a base at 30 mbar. We find that the optical depth is 0.5 at normal viewing geometry at a wavelength of 1 μm. Based on this calculated value, we then determine normal optical depths for our other condensates, if they were to form at this pressure, using equation (8). We also calculated the slant optical depths for HD 209458b, assuming $\eta = 66$. These are listed in Table 2. The f values for each condensate is the f of the limiting atomic species for each condensate, as given for 'Solar system abundances' in Lodders (2003). This assumes that there are no other molecules tying up the atoms, an assumption that is accurate at these high temperatures. The slant optical depths calculated are of the order of ∼0.1–1, meaning that their opacity is not negligible. From this analysis we can see that these minor condensates may well mask absorption features due to gaseous atomic and molecular species. In addition, if the atmospheres of transiting planets are enhanced in heavy elements these optical depths could well be larger. Jupiter's atmosphere is enhanced in heavy elements by a factor of about 3 over solar composition (Atreya et al. 2003) and Saturn's methane abundance has recently been pinned at ∼7 times solar (Flasar et al. 2005).

Non-equilibrium hazes, such as the photochemically produced hydrocarbon hazes found in the atmospheres of Jupiter, Saturn, Uranus, Neptune, Titan and Los Angeles, have long been observed and modelled (e.g. for Jupiter Tomasko, Karkoschka & Martinek 1986; West, Strobel & Tomasko 1986; Rages, Beebe & Senske 1999). In Jupiter, these stratospheric hazes can have normal optical depths of a few tenths at high latitudes. The scaleheight of these hazes is generally similar to the scaleheight of the surrounding gas (Moses, Rages & Pollack 1995; Rages et al. 1999).

To date, only Liang et al. (2004) have studied whether photochemically produced hydrocarbon hazes will be found in Pegasi planet atmospheres. These authors found it very unlikely that Pegasi planets would have hazes of this sort, due to several reasons. These include a lack of methane to be photolized (CO is the dominant carbon carrier), the high atmospheric temperatures, which would not allow any hydrocarbon products that were formed to condense and fast reverse reactions that quickly break down hydrogenated carbon compounds. However, these authors acknowledge that they do not consider ion-neutral chemistry, and they also note that the stellar wind could be a vast source for high-energy charged particles. Much work still needs to be done to definitively rule out hazes not predicted by equilibrium chemistry. Even condensates that form relatively thin hazes could have important effects on transmission spectroscopy.

4 DISCUSSION AND CONCLUSIONS

In our calculations we have used a relatively simple atmosphere model. We assume that the limb of the planet is uniform around the entire planet and that the atmosphere has a uniform *P–T* profile. It is certainly possible that this condition will not be met in reality (see Showman & Guillot 2002; Cho et al. 2003; Barman, Hauschildt & Allard 2005; Cooper & Showman 2005). As Iro et al. (2005) showed in the region of the 589-nm sodium doublet, it is possible for 'hot' and 'cold' limbs of a planet to show significantly different transmission signatures. Our main argument will likely hold even if the distribution of condensates is more complex than we have assumed. For instance, if the temperature on the limb simply monotonically increases from the night to day sides, one could imagine a series of atmosphere profiles where a given condensation curve is crossed at progressively lower pressures. At a given pressure at the terminator, this could lead to a lower condensate slant optical depth on the night side, but a higher slant optical depth on the day side, relative to our treatment here. It is certainly possible that different condensates could be important in different locations in a planet's atmosphere.

In this paper, we have taken a straightforward look at the optical depth that minor condensates may have in the slant viewing geometry relevant to planetary transits. While our findings are potentially not unanticipated, we felt the need to discuss this issue because the impact of minor condensates on the transit characterization of planetary atmospheres had not been discussed in the extrasolar planet literature to date. Our conclusions can be summarized as follows.

(i) For the *slant* viewing geometry relevant to transmission spectroscopy observations of EGPs, the slant optical depth can be of the order of 35–90 times larger than the normal optical depth. This depends upon the scaleheight of the condensate specifically, which may be smaller than the scaleheight of the surrounding gas.

(ii) Constraints on cloud location and thickness, and/or constraints on chemical abundances, obtained from transmission spectroscopy will not map directly on to constraints for the atmosphere when viewed at normal geometry. A cloud can be optically thick at slant viewing geometry and optically thin at normal viewing geometry. Thus, there could be abundant atomic Na and CO in the atmosphere of HD 209458b, even though Charbonneau et al. (2002) observed only a weak Na absorption feature, and Deming et al. (2005) observed no CO. The obscuring opacity source for this planet could be condensed Cr, MnS, silicates or Fe, and will depend on the actual temperatures on the planet's limb.

(iii) Minor equilibrium condensates or photochemically derived hazes that may be reasonably ignored for normal viewing geometry due to their low optical depths may have to be taken into account at slant viewing geometry.

(iv) These minor condensates may include ones we could reasonably predict the location and distribution (such as MnS) with an accurate *P–T* profile and assumed chemical mixing ratios, and those that we may remain ignorant of, such as photochemically produced hazes, that may have negligible *normal* optical depths.

We assert that transmission spectroscopy will continue to yield abundances of expected chemical species far below those predicted for a 'clear' atmosphere, for HD 209458b, and for other planets that may be studied in the future.

ACKNOWLEDGMENTS

I thank K. Lodders for numerous helpful discussions and for sharing condensation data prior to publication. I thank M. S. Marley for comments on the manuscript and also D. Charbonneau, T. M. Brown, J. W. Barnes, C. S. Cooper and W. B. Hubbard for interesting discussions. J. J. F. is supported by an NRC Research Associateship.

REFERENCES

Ackerman A. S., Marley M. S., 2001, ApJ, 556, 872
Allard F., Hauschildt P. H., Alexander D. R., Tamanai A., Schweitzer A., 2001, ApJ, 556, 357
Atreya S. K., Mahaffy P. R., Niemann H. B., Wong M. H., Owen T. C., 2003, Planet Space Sci., 51, 105
Barman T. S., Hauschildt P. H., Schweitzer A., Stancil P. C., Baron E., Allard F., 2002, ApJ, 569, L51
Barman T. S., Hauschildt P. H., Allard F., 2005, ApJ, in press (astro-ph/0507136)
Brooke T. Y., Knacke R. F., Encrenaz T., Drossart P., Crisp D., Feuchtgruber H., 1998, Icarus, 136, 1
Brown T. M., 2001, ApJ, 553, 1006
Carlson B. E., Lacis A. A., Rossow W. B., 1994, J. Geophys. Res., 99, 14623
Chamberlain J. W., Hunten D. M., 1987, International Geophysics Series, Vol. 36. Academic Press, Orlando
Charbonneau D., Brown T. M., Latham D. W., Mayor M., 2000, ApJ, 529, L45
Charbonneau D., Brown T. M., Noyes R. W., Gilliland R. L., 2002, ApJ, 568, 377
Cho J. Y.-K., Menou K., Hansen B. M. S., Seager S., 2003, ApJ, 587, L117
Cooper C. S., Showman A. P., 2005, ApJ, 629, L45
Cooper C. S., Sudarsky D., Milsom J. A., Lunine J. I., Burrows A., 2003, ApJ, 586, 1320
Deming D., Brown T. M., Charbonneau D., Harrington J., Richardson L. J., 2005, ApJ, 622, 1149
Fegley B. J., Lodders K., 1994, Icarus, 110, 117
Flasar F. M. et al., 2005, Sci, 307, 1247
Fortney J. J., Sudarsky D., Hubeny I., Cooper C. S., Hubbard W. B., Burrows A., Lunine J. I., 2003, ApJ, 589, 615
Fortney J. J., Marley M. S., Lodders K., Saumon D., Freedman R., 2005, ApJ, 627, L69
Harrington J., Deming D., Matthews K., Richardson L. J., Rojo P., Steyert D., Wiedemann G., Zeehandelaar D., 2002, BAAS, 34, 1175
Haywood J., Gibb E., Brittain S., Rettig T., Kulesa C., 2004, AAS/Division for Planetary Sciences Meeting Abstracts, 36
Henry G. W., Marcy G. W., Butler R. P., Vogt S. S., 2000, ApJ, 529, L41
Hubbard W. B., Fortney J. J., Lunine J. I., Burrows A., Sudarsky D., Pinto P., 2001, ApJ, 560, 413
Iro N., Bezard B., Guillot T., 2005, A&A, 436, 719
Liang M., Seager S., Parkinson C. D., Lee A. Y.-T., Yung Y. L., 2004, ApJ, 605, L61
Lodders K., 2003, ApJ, 591, 1220
Lodders K., Fegley B. 2005, Astrophys. Update, in press
Marley M. S., 2000, in Griffith C. A., Marley M. S., eds, ASP Conf. Ser. Vol. 212, From Giant Planets to Cool Stars. Astron. Soc. Pac., San Francisco, p. 152
Marley M. S., Seager S., Saumon D., Lodders K., Ackerman A. S., Freedman R. S., Fan X., 2002, ApJ, 568, 335
Marley M. S., Cushing M. C., Saumon D., 2005, in Favata F., Hussain G., Battrick B., eds, Proc. ESA SP-560, Proc. 13th Cool Stars Workshop. ESA Publications Division, Noordwijk, p. 791
Moses J. I., Rages K., Pollack J. B., 1995, Icarus, 113, 232
Narita N. et al., 2005, PASJ, 57, 471
Rages K., Beebe R., Senske D., 1999, Icarus, 139, 211
Seager S., Sasselov D. D., 2000, ApJ, 537, 916
Showman A. P., Guillot T., 2002, A&A, 385, 166
Sudarsky D., Burrows A., Hubeny I., 2003, ApJ, 588, 1121
Tomasko M. G., Karkoschka E., Martinek S., 1986, Icarus, 65, 218
Vidal-Madjar A., Lecavelier des Etangs A., Désert J.-M., Ballester G. E., Ferlet R., Hébrard G., Mayor M., 2003, Nat, 422, 143
Vidal-Madjar A. et al., 2004, ApJ, 604, L69
West R. A., Strobel D. F., Tomasko M. G., 1986, Icarus, 65, 161

This paper has been typeset from a TEX/LATEX file prepared by the author.